

Dynamic Stress Intensity Factors during Viscoelastic Crack Propagation at Various Strain Rates

AKIRA KOBAYASHI, NOBUO OHTANI, and MASAYUKI MUNEMURA,
*Institute of Space and Aeronautical Science, University of Tokyo, Komaba,
Meguro-ku, Tokyo, 153, Japan*

Synopsis

Dynamic stress intensity factors K_D were measured by the caustic method and crack propagation velocity \dot{C} by the velocity gauge techniques for PMMA [poly(methyl methacrylate)] during dynamic crack propagation at various strain rates $\dot{\epsilon}$. No definite applied strain rate effects on the dynamic stress intensity factor were observed for applied strain rates ranging from 8.33×10^{-4} to 30/sec; however, the test results do show crack propagation velocity dependency in $K_D \sim \dot{C}$ relations. The high local strain rate region may be realized at the running crack tip even under the quasi-static loading case of $\dot{\epsilon} = 8.33 \times 10^{-4}$ /sec, since all the crack propagation velocities obtained were greater than 50 m/sec even up to 450 m/sec.

INTRODUCTION

The caustic or shadow spot method, first employed for crack propagation by Manogg¹ and Theocariz,² is a powerful tool for measuring the dynamic stress intensity factors experimentally in the course of running crack propagation in solids.

In the present report, the dynamic stress intensity factors during crack propagation in a viscoelastic solid such as PMMA [poly(methyl methacrylate)] are measured using a caustic method at various strain rates $\dot{\epsilon}$.

EXPERIMENTAL

Specimens

The test material is a commercial PMMA [poly(methyl methacrylate)], Sumipex (manufactured by Sumitomo Chemical Co., Japan) and is machined into a specimen configuration as shown in Figure 1. The crack initiation notch is

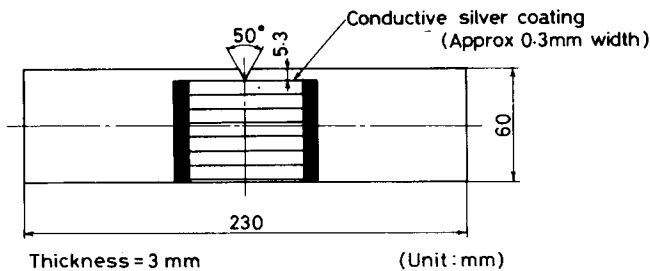


Fig. 1. Test specimen. Thickness = 3 mm.

prepared by fatigue of approximate 10^3 cycles. Conductive silver-coated material (du Pont No. 4817) was applied on the specimen surface as velocity gauges³ to measure the propagation velocity of a running crack. For further details refer to a previous article.³

Experimental Procedures

For lower strain rates, these test specimens were subjected to tension until unstable fracture initiation began by a conventional Instron-type tester at room temperature. For higher strain rates of about 30/sec, the drop-weight type was employed, as shown in Figure 2. During all the experiments, load was measured by a load cell for lower strain rates and by a strain gauges for higher strain rates, crack propagation velocities by velocity gauges, and dynamic stress intensity factors by the caustic method. All the tests were performed at room temperatures of about 25°C.

Caustic Method

Actual dynamic stress intensity factors were measured by the caustic method in combination with a Cranz-Schardin-type high-speed camera (Chronolite, Impulsphysik GmbH of West Germany). The optical arrangement for the caustic method is shown in Figure 3.

Measurement of a diameter, D , of an obtained shadow pattern bound by bright light, which is the caustic observed on a screen placed behind the specimen, leads to the dynamic stress intensity factor K_D , which is given by⁴

$$K_D = \frac{1.671}{z_0 t C_t \lambda^{3/2}} \left(\frac{D}{3.16} \right)^{5/2}$$

where K_D is the dynamic stress intensity factor, D is the diam. of the caustic, z_0

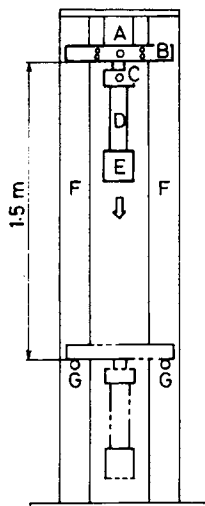


Fig. 2. Drop-weight-type loading system. (A) magnet; (B) loading bar; (C) jaw for gripping; (D) test specimen; (E) jaw and weight; (F) guide; (G) stopper.

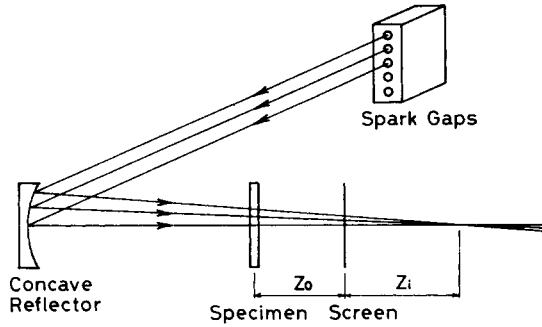


Fig. 3. Optical arrangement for the caustic method.

is the distance between the specimen and the screen and is 220 mm, z_i is the distance between the focus and the screen measuring 550 mm, t is the specimen thickness = 3 mm, λ is the $z_i/(z_0 + z_i)$, and C_t is the stress optical coefficient = $0.48 \times 10^{-3} \text{ mm}^2/\text{kg}$.

A schematic diagram of experimental measurement is shown in Figure 4.

RESULTS AND DISCUSSIONS

An example of a shadowgraph observed in PMMA by the caustic method is shown in Figure 5.

During the dynamic crack propagation, the load was monitored by a load cell for lower strain rates of $\dot{\epsilon} = 8.33 \times 10^{-4}/\text{sec}$ and $\dot{\epsilon} = 8.33 \times 10^{-2}/\text{sec}$, and by strain gauges for $\dot{\epsilon} = 30/\text{sec}$, resulting in almost constant load throughout the crack propagation for individual cases, respectively. The lower strain rates of $\dot{\epsilon} = 8.33 \times 10^{-4}/\text{sec}$ and $\dot{\epsilon} = 8.33 \times 10^{-2}/\text{sec}$ are prescribed by $\dot{\epsilon} = V/L_0$, where V is a

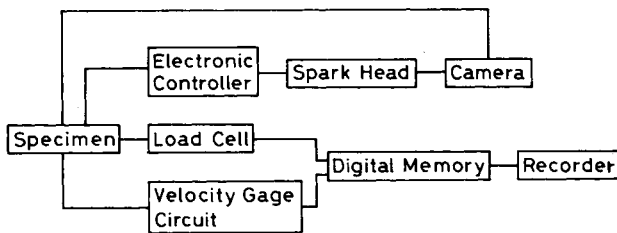


Fig. 4. Schematic diagram for experimental measurements.

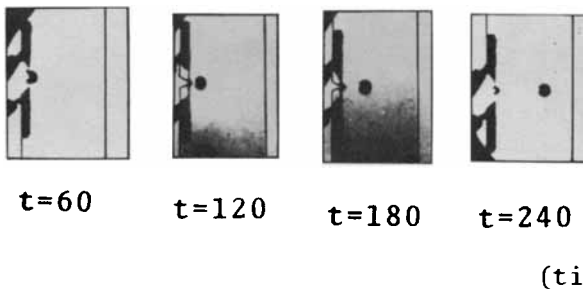


Fig. 5. An example of a shadowgraph: $\dot{\epsilon} = 8.33 \times 10^{-4}/\text{sec}$, time is in μsec ; $t = 60, 120, 180, 240$, respectively.

crosshead speed and L_0 is a distance between jaws for gripping and the higher strain rate of $\dot{\epsilon} = 30/\text{sec}$ is obtained by a strain-gauge recording.

The applied load is maintained at almost constant throughout the crack propagation, this indicates an unstable dynamic crack propagation. In such an unstable crack propagation in a viscoelastic solid, the brittleness becomes more prevailing as the applied strain rates increase.³ Therefore, correlations are expected between the dynamic stress-intensity factor and the applied strain rate.

The obtained K_D values as a function of crack velocity \dot{C} at various strain rates are shown in Figure 6 where $C_t = 0.48 \times 10^{-3} \text{ mm}^2/\text{kg}$. This dynamic case value is employed for all strain rate cases, since the crack propagation velocity \dot{C} is greater than 100m/sec, even for the quasistatic case of $\dot{\epsilon} = 8.33 \times 10^{-4}/\text{sec}$.

The K_D values in Figure 6 do not show conspicuous differences due to applied strain rates. Thus, K_D is independent of applied strain rates, contrary to expectation. K_D (Fig. 6) increases with an increase in \dot{C} , as observed by Theocaris and Katsamanis⁴ and Green⁵; but they did not investigate the applied strain rate effect. However, no definite strain rate dependency is observed for the present $K_D \sim \dot{C}$ curve. The strain rates (Fig. 6) are measured as average values prescribed for the distance between jaws for gripping for lower strain rates and for the strain gauge length for a higher strain rate case. Therefore, the very strain rate actually realized at a crack tip must be of far greater value than those prescribed for the distance between jaws for gripping or for the strain gauge length.

Evidence is given by Williams' theoretical analysis⁶ which shows that the strain rate as high as $\dot{\epsilon} = 2 \times 10^5/\text{sec}$ is calculated at the crack tip for $\dot{C} = 50 \text{ m/sec}$. In the present experiment, $\dot{C} = 50 \sim 450 \text{ m/sec}$ is observed, so the strain rate at the running crack tip must be very high.⁶ Actually, Williams' analysis is within the linear elastic fracture mechanics; the present experimental case, however, is of viscoelastic fracture, and may not exhibit such high strain rate values at the crack tip as expected by Williams' analysis. Nevertheless, the strain rate at the running crack tip must be very high even for the lower strain rate of $8.33 \times 10^{-4}/\text{sec}$, since the crack propagation velocity is very fast.

In the dynamic photoelastic experimental study⁷ for epoxy resin, the principal stress differences around the running crack tip for $\dot{\epsilon} = 38/\text{sec}$ are similar to those for $\dot{\epsilon} = 5 \times 10^{-4}/\text{sec}$ in both values and distributions, suggesting no major differences in dynamic stress intensity factors.

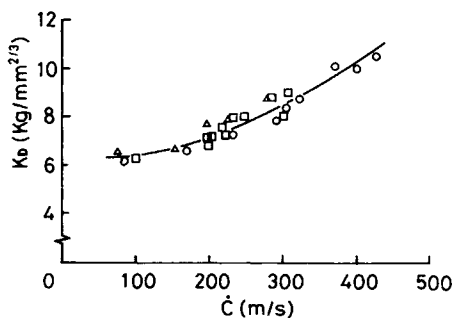


Fig. 6. Dynamic stress intensity factors vs. dynamic crack propagation velocity. (O) 8.33×10^{-4} ; (\square) 8.33×10^{-2} ; (Δ) ≈ 30 ; $\dot{\epsilon}$ in sec^{-1} .

CONCLUSION

The applied strain rate effects on dynamic stress-intensity factors was not observed. Further efforts to investigate the local strain rate at the running crack tip might explain the present results.

The authors thank Mr. Haruo Kobayashi, Mr. Kenji Kodama, and Mr. Yoshinari Fujii for their assistance in the present work.

References

1. P. Manogg, *Proceedings of the International Conference on Physics of Non-Crystalline Solids*, Delft, Netherlands, 1964, p. 481.
2. P. S. Theocaris, *Trans. ASME, Ser. E*, **37**, 409 (1970).
3. A. Kobayashi, N. Ohtani, and T. Sato, *J. Appl. Polym. Sci.*, **18**, 1625 (1974).
4. P. S. Theocaris and F. Katsamanis, *Eng. Frac. Mech.*, **10**, 197 (1978).
5. A. K. Green, Ph.D. thesis, Imperial College, London University, England, 1971.
6. J. G. Williams, *Int. J. Fract. Mech.*, **8**, 393 (1972).
7. A. Kobayashi, T. Sato, and N. Ohtani, *Bull. Inst. Space Aero. Sci.*, Univ. of Tokyo, Jpn., **10**, 835 (1974).

Received February 18, 1980

Accepted May 23, 1980